

# Modulation of Adipose Tissue Expression of Murine Matrix Metalloproteinases and Their Tissue Inhibitors With Obesity

Erik Maquoi,<sup>1</sup> Carine Munaut,<sup>2</sup> Alain Colige,<sup>3</sup> Désiré Collen,<sup>1</sup> and H. Roger Lijnen<sup>1</sup>

**The potential role of the matrix metalloproteinase (MMP) system in the pathophysiology of the adipose tissue was investigated in a mouse model of nutritionally induced obesity. mRNA levels of 16 MMPs and 4 tissue inhibitors of MMPs (TIMPs) were measured by semiquantitative RT-PCR in adipose tissue isolated from mice maintained for 15 weeks on a standard or high-fat diet. In mice on standard diet, with the exception of MMP-8, all MMP and TIMP transcripts were detected in both gonadal and subcutaneous depots. In obese mice, the expression of MMP-3, -11, -12, -13, and -14 and TIMP-1 mRNAs was upregulated, whereas that of MMP-7, -9, -16, and -24 and TIMP-4 was downregulated. Most MMP and TIMP mRNAs were expressed at higher levels in stromal-vascular cells than in mature adipocytes. Analysis of adipose tissue by in situ fluorescent zymography revealed MMP-dependent proteolytic activities, demonstrating the presence of active MMPs in the intact tissue. In vitro conversion of adipogenic 3T3-F442A cells into mature adipocytes was associated with substantial modulations of MMP and TIMP expression. Moreover, this in vitro adipogenesis was reduced in the presence of a synthetic MMP inhibitor. Thus, the adipose tissue expresses a large array of MMPs and TIMPs, which modulate adipocyte differentiation. *Diabetes* 51:1093–1101, 2002**

**A**dipose tissue is composed of lipid-filled cells (adipocytes) surrounded by collagen fibers, blood vessels, nerves, fibroblasts, and immune cells. Until recently, white adipose tissue was considered an inert fat-storing tissue. However, recent findings demonstrated that they play a dynamic role in the highly regulated uptake, storage, and release of lipids. Moreover, adipose tissue secretes several molecules, including sex steroids, glucocorticoids, hormone precursors,

and cytokines, suggesting that it should be considered an endocrine organ (1).

The chronic imbalance between energy intake and expenditure results in obesity, a pathological condition of the adipose tissue that is characterized by an excess of fat mass resulting from an increase in the number and size of the adipocytes (2,3). In most Western societies, obesity has reached epidemic proportions and constitutes an increased risk for the development of several pathologies, including type 2 diabetes, insulin resistance, cardiovascular disease, and atherosclerosis (4,5).

Development of obesity is associated with an extensive reorganization of the adipose tissue that involves adipogenesis, angiogenesis, and remodeling of the extracellular matrix (ECM) (6). Two major proteolytic systems, the serine proteinases and matrix metalloproteinases (MMPs), have been implicated in several pathophysiological processes involving extensive ECM remodeling (7). Plasminogen activator inhibitor-1 (PAI-1), the primary inhibitor of tissue-type and urokinase-type plasminogen activators, is highly expressed in adipose tissue of obese mice and humans (8,9), suggesting a role for this proteinase family in the adipose tissue. In contrast, little is known of the potential involvement of MMPs in the physiology and pathology of fat tissue.

The MMPs belong to a family of >23 neutral endopeptidases that are collectively able to cleave all of the ECM components as well as several non-ECM proteins, such as adhesion molecules, cytokines, proteinase inhibitors, and other MMPs (10–12). MMPs are highly regulated enzymes with expression, secretion, and activity levels under tight control (13). In most cases, MMPs are expressed at very-low levels; however, expression is rapidly induced at times of active tissue remodeling. MMPs are synthesized as latent precursors that have to be proteolytically activated to generate fully mature enzymes. MMP activity is further modulated through interactions with tissue inhibitors of MMPs (TIMPs) (14). Four TIMPs have been characterized and most are able to inhibit the activities of all known MMPs. Consequently, the net MMP activity in tissues is locally determined by the balance between the levels of activated MMPs and TIMPs.

It is generally accepted that alterations in gene expression may contribute to the pathogenesis of obesity. To gain further insight into the involvement of the MMPs in the pathophysiology of adipose tissue, we monitored the expression of MMPs and TIMPs in an in vivo mouse model

From the <sup>1</sup>Center for Molecular and Vascular Biology, University of Leuven, Belgium; the <sup>2</sup>Laboratory of Tumor and Development Biology, University of Liège, Belgium; and the <sup>3</sup>Laboratory of Biology of Connective Tissues, University of Liège, Belgium.

Address correspondence and reprint requests to H.R. Lijnen, Center for Molecular and Vascular Biology, University of Leuven, Campus Gasthuisberg, O & N, Herestraat 49, B-3000 Leuven, Belgium. E-mail: roger.lijnen@med.kuleuven.ac.be.

Received for publication 7 September 2001 and accepted in revised form 8 January 2002.

DMEM, Dulbecco's modified Eagle's medium; ECM, extracellular matrix; GPDH, glycerophosphate dehydrogenase; HFD, high-fat diet; KRBB, Krebs-Ringer bicarbonate buffer; MMP, matrix metalloproteinase; PAI-1, plasminogen activator inhibitor-1; PPAR, peroxisome proliferator-activated receptor; SFD, standard-fat diet; S-V, stromal-vascular; T<sub>3</sub>, triiodothyronine; TIMP, tissue inhibitor of MMP.

of nutritionally induced obesity as well as in an in vitro model of adipogenesis.

## RESEARCH DESIGN AND METHODS

**Experimental protocol.** Five-week-old male wild-type mice (mixed 75% C57/BL6:25% 129Svj genetic background) were maintained on a standard-fat diet (SFD) (4% [wt/wt] fat,  $n = 11$ ) or given a high-fat diet (HFD) (21% [wt/wt] fat coming from milk fat, and 49% [wt/wt] carbohydrate coming from sucrose and corn starch,  $n = 11$ ) (Harlan TD 88137; Harlan, Zeist, the Netherlands) for 15 weeks. The SFD contained 13% kcal as fat, and the HFD contained 42% kcal as fat. After fasting overnight, the mice were weighed and killed with an overdose (60 mg/kg i.p.) of Nembutal (Abbott Laboratories, North Chicago, IL). Intra-abdominal (gonadal) and inguinal subcutaneous fat pads were removed and weighed. Fat pads were either prepared for histology or immediately frozen in liquid nitrogen and stored at  $-80^{\circ}\text{C}$ . Blood samples were obtained from the retroorbital sinus, and glucose concentrations were measured with Glucocard strips (Menarini Diagnostics). All animal experiments were approved by the local ethical committee and performed in accordance with the guiding principles of the American Physiological Society and the International Society on Thrombosis and Hemostasis (15).

**Histological analysis.** The mean diameter of adipocytes was determined by computer-assisted image analysis (Quantimed 600; Leica, Hamburg, Germany) in 15- $\mu\text{m}$  frozen-cut adipose tissue sections stained with hematoxylin-eosin. For each animal, three to four sections were analyzed (four fields per section) and averaged.

In situ fluorescent zymography of cryosections of adipose tissue using casein- or gelatin-containing gels was performed essentially as described (16). The substrate gel (0.5% agarose) contained 1 mg/ml resorufin-labeled casein (Boehringer Mannheim, Mannheim, Germany) or pig skin gelatin Oregon Green-488 conjugate (Molecular Probes Europe BV, Leiden, the Netherlands). Overlays were analyzed by fluorescent microscopy after 48 h incubation at  $37^{\circ}\text{C}$ ; lysis of the substrate gel was expressed in percent of section area.

**Adipose tissue dissociation.** Pooled gonadal or subcutaneous fat pads dissected from mice maintained on SFD ( $n = 5$ ) or HFD ( $n = 4$ ) were used to separate mature adipocytes from stromal-vascular (S-V) cells by collagenase treatment (17). Briefly, minced fat pads were digested in Krebs-Ringer bicarbonate buffer (KRBB) (Sigma Chemicals, St. Louis, MO) (pH 7.3) supplemented with 3% (wt/vol) albumin (KRBB-BSA) and 1.5 mg/ml collagenase (Sigma) at  $37^{\circ}\text{C}$  for 1 h. Undigested tissue fragments were removed by filtration through a 250- $\mu\text{m}$  nylon screen. Adipocytes were separated by their ability to float on low-speed centrifugation. The floating fat cells were resuspended in KRBB-BSA, washed, and centrifuged as described above. The first and second pellets containing S-V cells were pooled. Erythrocytes contaminating the S-V fraction were eliminated using Red Blood Cell Lysis Buffer (Roche Molecular Biochemicals, Mannheim, Germany) according to the manufacturer's instructions. The two cell populations were washed and resuspended in PBS.

**Culture and differentiation of 3T3-F442A cells.** 3T3-F442A preadipocytes (gift from Prof. R. Négrel, University of Nice, France) were routinely grown in basal medium: Dulbecco's modified Eagle's medium (DMEM)/nutrient mix F12 (1:1) (Life Technologies, Merelbeke, Belgium) containing 100 mmol/l pantothenate, 1 mmol/l biotin, 2.5 mmol/l glutamine, and 15 mmol/l HEPES, supplemented with 10% (vol/vol) FBS (fetal bovine serum) (Life Technologies). To induce differentiation, cells were seeded at  $3.6 \times 10^4$  cells/cm<sup>2</sup> and grown to confluence in basal medium with 10% FBS. Confluent cultures (day 0) were washed in serum-free basal medium and treated for 5 days with an induction medium: basal medium supplemented with BSA (100 mg/l), ITS (10 mg/l insulin, 5.5 mg/l transferrin, and 5  $\mu\text{g/l}$  selenium) (Sigma), 10 nmol/l dexamethasone, 250  $\mu\text{mol/l}$  methylisobutylxanthine, and 1 nmol/l triiodothyronine ( $T_3$ ). Cultures were then switched to a differentiation medium (basal medium supplemented with ITS and  $T_3$ ) for 2 weeks (induction and differentiation media were renewed every 2–3 days). The influence of MMP inhibition on in vitro adipogenesis was investigated by supplementing both induction and differentiation media with either vehicle (0.05% DMSO) (Sigma) or a synthetic MMP inhibitor (0.1–10  $\mu\text{mol/l}$  CT1746) (CellTech, Slough, U.K.). Cellular viability was assessed by cell counting, Trypan Blue dye exclusion assay, and WST-1 assay (Roche Molecular Biochemicals) as previously described (18). Briefly, cells that were or were not treated with CT1746 were supplemented with WST-1 tetrazolium salt (10% vol/vol) and incubated for 2 h at  $37^{\circ}\text{C}$ . WST-1 is cleaved to formazan by the mitochondrial dehydrogenases of metabolically active cells. Accumulation of formazan was quantified by spectrophotometry.

Total RNAs and conditioned media were collected at various time points during the differentiation process. Secretion of MMP-2, MMP-9, and TIMPs

into the culture medium was evaluated by gelatin zymography and reverse zymography, respectively, as previously described (18,19).

**Flow cytometric analysis.** To assess the extent of preadipocyte differentiation, cytosolic triglyceride content was quantified by determining Nile Red uptake. Cells were harvested by treatment with trypsin (0.5 g/l), EDTA (0.2 g/l), and collagenase (2 g/l) in Hank's balanced salt solution at  $37^{\circ}\text{C}$ , washed in DMEM/nutrient mix F12 containing 10% FBS, and incubated for 10 min in PBS containing Nile Red (10  $\mu\text{g/ml}$ ) (Molecular Probes). Cells were subjected to flow cytometric analysis (FACSCalibur; Becton Dickinson, Aalst, Belgium) with 20,000 events collected per sample, as described (20). The 488-nm excitation light was used to generate forward scatter and right-angle scatter signals. Nile Red fluorescence was detected at 530 nm, and data were expressed as a contour plot.

**RNA isolation.** DNA-free total RNAs were extracted from frozen adipose tissue (gonadal and subcutaneous) as well as from isolated adipocytes, S-V cells, and 3T3-F442A cells by the HighPure RNA tissue and HighPure RNA isolation kits (Roche Molecular Biochemicals), respectively, according to the manufacturer's instructions. RNA concentrations were measured using the RiboGreen RNA quantification kit (Molecular Probes). Total RNA samples were diluted in water and stored at  $-80^{\circ}\text{C}$ .

**Oligonucleotide primers.** The design of oligonucleotide primers specific for the different targets was based on sequences available in the GenBank (Table 1). When the genomic sequence of the targets was available, primers (Eurogentec, Seraing, Belgium) annealing to distinct exons were selected in order to discriminate between RT-PCR products resulting from the amplification of the target mRNA or from contaminating genomic DNA. The specificity of the different primer pairs was tested by subjecting RNA isolated from known positive control tissue to RT-PCR (Table 1). RT-PCR products were cloned into a pCRII-TOPO vector (Invitrogen, Groningen, the Netherlands) according to the manufacturer's instructions and cycle sequenced with M13R primer (Invitrogen) on a GeneAmp 9700 thermal cycler using the BigDye Terminator Cycle Sequencing Kit (Applied Biosystems, Nieuwerkerk a/d IJssel, the Netherlands). The PCR products were separated and analyzed on an ABI Prism 310 Genetic Analyzer (Applied Biosystems). The identity of the resulting sequences was verified with the NCBI BLASTN program.

**Semiquantitative RT-PCR.** The expression level of the different RNAs was determined by semiquantitative RT-PCR. RT reactions were performed from 10 ng total RNA with thermostable RT (*rTh*) at  $70^{\circ}\text{C}$  for 15 min using the GeneAmp Thermostable RNA PCR Kit (Applied Biosystems) and target-specific antisense primers (Table 1). PCR amplifications were performed with target-specific sense primers (Table 1). The reactions were run for the corresponding number of cycles (Table 1) in a GeneAmp 9700 thermal cycler. The number of cycles was optimized for each target so that the PCR products did not reach plateau levels. RT-PCRs without sample were used as negative controls. RT-PCR products were separated on 10% acrylamide gels and stained with SYBR Green (Molecular Probes). The intensities of the bands were quantified with the Gel Doc 2000 System using Quantity One software (Bio-Rad, Eke, Belgium). To normalize the mRNA levels in the different samples, the intensity of the band corresponding to each mRNA was divided by the intensity of the band corresponding to the 28S rRNA, which was used as an internal standard.

**Statistical analysis.** Data were reported as means  $\pm$  SE, and statistical analysis was performed by Student's *t* test. The correlations between mRNA levels and adipose tissue weights were examined using the nonparametric Spearman's rank correlation coefficient test. Thresholds for significance were set at  $P < 0.05$ .

## RESULTS

**Nutritionally induced obesity in mice.** Mice maintained on HFD for 15 weeks had a significantly higher total body weight than age-matched mice on SFD, and the weight of their gonadal and subcutaneous fat pads was significantly higher (Table 2). Expressed in percent of the total body weight, gonadal fat represents  $4.9 \pm 0.34\%$  for mice on HFD as compared with  $1.1 \pm 0.10\%$  for mice on SFD ( $P < 0.000001$ ); corresponding values for subcutaneous fat are  $4.6 \pm 0.29\%$  vs.  $1.0 \pm 0.14\%$  ( $P < 0.000001$ ). The mean diameter of the adipocytes was higher in both gonadal and subcutaneous fat depots of mice on HFD (Table 2). The HFD significantly increased blood glucose levels (Table 2). **Expression of MMPs and TIMPs in adipose tissue of lean mice.** Gonadal and subcutaneous depots isolated

TABLE 1  
Sequence of primers used for the RT-PCR assays

RNA species*	Primers (5'-3')		Product size (bp)	Positive control	Cycling profile†	Cycle number‡
	Sense	Antisense				
MMP-2 (M84324)	AGATCTTCTTCTTCAA GGACCGGTT	GGCTGGTCAGTGGCTTGG GGTA	225	Lung	A	30/30/31
MMP-3 (X66402)	GATCTTTCATTTTG GCCATCTCTTC	CTCCAGTATTTGTCTCTA CAAAGAA	246	Lung	B	48/40/41
MMP-7 (L36244)	GCGGAGATGCTCAC TTTGACA	ATTCATGGGTGGCAGCA AAC	87	Uterus	A	35/43/42
MMP-8 (NM_008611)	CCAAGTGGGAACGC ACTAACTTGA	TGGAGAATTGTCACCGT GATCTCTT	200	Lung	A	45/50/45
MMP-9 (NM_013599)	CCCACATTTGACGTC CAGAGAAGAA	GTTTTTGTGCTATTGCT GAGATCCA	208	Brain	B	44/39/41
MMP-10 (Y13185)	TCCCGAGCCTGAAT TTCAT	AGCCTCATAGGCAGCAT CTAA	76	Small Intestine	C	48/47/41
MMP-11 (Z12604)	ATTTGGTTCTTCCA AGGTGCTCAGT	CCTCGGAAGAAGTAGATC TTGTTCT	155	3T3 cells	B	38/34/33
MMP-12 (NM_008605)	ACATTTGCGCTCTC TGCTGATGAC	CAGAAACCTTCAGCCAGAA GAACC	201	Lung	A	34/35/42
MMP-13 (NM_008607)	ATGATCTTTAAAGA CAGATTCTTCTGG	TGGGATAACCTTCCAGAAT GTCATAA	203	3T3 cells	B	39/36/38
MMP-14 (NM_008608)	GGATACCCAATGCC CATTGGCCA	CCATTGGGCATCCAGAAG AGAGC	221	Liver	A	28/26/21
MMP-15 (D86332)	GGTACATGTGAAAG CCAACCT	GTACCAGCCCAGCTTCT CAG	121	Lung	C	45/41/45
MMP-16 (NM_019724)	GTAACCTCCAAAAGT TGGAGATCCTG	TCTAATTCAGTGTAGGGAA CTTCTTCAA	113	Brain	C	31/33/34
MMP-17 (AB021224)	GCCGGGATACTGTG CGT	CTACCTCGTGGAAGTTCA AGG	81	Brain	C	28/28/32
MMP-19 (AF155221)	TGGGCCACTGGAGA AAGAAG	TCAGCCCAACCAGCTTT CAC	157	Lung	C	28/27/24
MMP-23 (AF085742)	TTCCCCATTCAGTTT CCGTG	AAGAAAGCGTGGGCCA GTT	147	Heart	C	35/34/35
MMP-24 (AJ010262)	AGGCTATTCGTCAGG CTTTC	TTTTGATCTCATGGTAT GGCA	81	Brain	C	45/44/41
TIMP-1 (X04684)	GGCATCCTCTTGTTG CTATCACTG	GTCATCTTGATCTCATAA CGCTGG	174	3T3 cells	A	31/32/30
TIMP-2 (NM_011594)	CTCGCTGGACGTTGG AGGAAAAGAA	AGCCCATCTGGTACCTGT GGTTCA	161	3T3 cells	A	23/22/23
TIMP-3 (NM_011595)	CTTCTGCAACTCCGA CATCGTGAT	CAGCAGGTACTGGTACTT GTTGAC	216	Lung	A	25/25/45
TIMP-4 (AI551619)	ACTTGCTATGCAGTG CCATG	TCGGTACCAGCTGCAGATG	144	Brain	C	26/28/34
vWF (U27810)	GGTCAGACGAAGTTG GTGAAG	CCCCATTGAAGGCATACTCC	150	Lung	C	-/48/-
Pref-1 (L12721)	AACCATGGCAGTGCA TCTG	AGCATTCGTAAGGCCTTTC	132	Preadip	C	-/-/26
GPDH (J02655)	GGTGGCAGAGGCCTTTG	TGCCCATTTAGCATCTCCTT	69	Adip	C	-/-/37
PPAR-γ (NM_011146)	CTGTGCGTTTCAGAAGT GCCT	CCCAAACCTGATGGCATTG TGAGACA	99	Adip	C	-/-/26
PAI-1 (M33960)	AGGGCTTCATGCCCC ACTTCTTCA	AGTAGAGGGCATTACCA GCACCA	197	Adip	A	-/-/27
28S rRNA (X00525)	GTTCACCCACTAATA GGGAACGTGA	GGATTCTGACTTAGAGGC GTTTCAGT	212	Lung	A	19/17/17

\*GenBank accession nos. of the targets are indicated in parentheses. †Cycle profiles A–C are as follows: after 120 s at 95°C, PCR mixtures were subjected to a cycle profile, including denaturation for 15 s at 94°C, annealing for 20, 30, and 20 s at 68, 63, and 60°C, extension for 10, 30, and 10 s (A, B, and C, respectively) at 72°C and a 2-min extension at 72°C for the last cycle. ‡Number of cycles used to amplify sequences in adipose tissue/isolated cell fractions/3T3 cells. Adip, adipocytes; preadip, preadipocytes; pref-1, preadipocyte factor-1; vWF, von Willebrand factor.

from 20-week-old mice maintained on SFD were analyzed by semiquantitative RT-PCR. Except for MMP-8, all 16 MMPs and 4 TIMPs analyzed were detected in both gonadal and subcutaneous adipose tissue (Fig. 1A). Although the expression levels of most mRNAs did not

markedly differ between gonadal and subcutaneous fat, the MMP-3 mRNA level was higher in subcutaneous than in gonadal fat, whereas MMP-24 mRNA was lower in the subcutaneous depot (Fig. 1A). However, the limited number of subcutaneous samples ( $n = 2$ ) obtained from lean

TABLE 2

Effect of 15 weeks of HFD on body weight and adipose tissue weight and cellularity

	SFD	HFD
Body weight (g)	28 ± 1.2	40 ± 1.4*
Blood glucose (mg/dl)†	92 ± 5.7	154 ± 19‡
GON fat		
Weight (g)†	0.31 ± 0.04	2.0 ± 0.18*
Adipocyte diameter (μm)§	42	83 ± 3
SC fat		
Weight (g)†	0.29 ± 0.05	1.9 ± 0.16*
Adipocyte diameter (μm)§	41	71 ± 2

Data are means ± SE. \* $P < 0.000001$  vs. SFD. †Totals of 10 and 11 determinations for SFD and HFD, respectively. ‡ $P < 0.01$  vs. SFD. §Mean of two determinations for SFD, and means ± SE of six determinations for HFD. GON, gonadal; SC, subcutaneous.

mice did not allow us to statistically compare the mRNA levels between subcutaneous and gonadal fat.

**Modulation of MMP and TIMP expression in fat pads by nutritionally induced obesity.** Next, we investigated the expression of MMPs and TIMPs in adipose tissue from mice maintained on HFD for 15 weeks. As for the lean mice, all mRNAs investigated, with the exception of MMP-8, were expressed in both gonadal and subcutaneous depots of obese mice (Fig. 1B). In gonadal adipose tissue, the HFD did not significantly affect the mRNA levels of MMP-2, -10, -15, -17, -19, and -23 and TIMP-2 and -3. In contrast, the expression of MMP-3, -11, -12, -13, and -14 and TIMP-1 was increased, whereas MMP-7, -9, -16, and -24 and TIMP-4 mRNA levels were downregulated (Fig. 1B). The limited number of subcutaneous fat samples ( $n = 2$ ) obtained from lean mice did not allow us to perform statistical analysis on the modulations of the mRNA levels induced by the HFD in that depot. Nevertheless, our data suggest that, with the exception of MMP-12, -13, and -15 and TIMP-1, modulations similar to those observed in gonadal fat also occurred in the subcutaneous depot (Fig. 1B).

**Cellular localization of MMP and TIMP mRNAs in adipose tissue.** Gonadal and subcutaneous depots were dissociated and mature adipocytes separated from the S-V cells by centrifugation. Total RNA was isolated from the resulting cell fractions and subjected to RT-PCR. Because adipocytes have been shown to be intimately associated with microvascular endothelial cells (21), we carefully assessed the potential contamination of the adipocytes with endothelial cells by determining the level of von Willebrand factor mRNA (a marker of endothelial cells). As expected, a specific band was observed in the S-V fractions after a high number of PCR cycles, confirming the presence of endothelial cells. Low expression levels (ranging from 0.5 to 20% of those observed in the corresponding S-V fractions) were also detected in some adipocyte fractions, indicating the presence of a low number of contaminating endothelial cells (Table 3).

In mice maintained on SFD, the expression of the different MMP and TIMP mRNAs in isolated cell populations was heterogeneous and, for some of them, different between gonadal and subcutaneous depots (Table 3). Schematically, MMPs and TIMPs can be classified into four groups based on their cellular distribution. A first group, characterized by high expression levels in S-V cells

and no or only marginal expression in adipocytes, comprises MMP-2, -9, -11, -13, -14, -16, and -23 and TIMP-1 and -2 (in both gonadal and subcutaneous fat), MMP-3, -7, and -17 (in gonadal fat), and MMP-10 and -12 (in subcutaneous fat). A second group, characterized by expression in both S-V cells and adipocytes, but at higher levels in the former, includes MMP-3 and -17 (in subcutaneous fat) and MMP-24 and TIMP-3 (in gonadal fat). A third group, characterized by similar expression levels in S-V cells and adipocytes, comprises MMP-10 (in gonadal fat), MMP-15, and TIMP-3 (both in subcutaneous fat). A fourth group, characterized by higher expression levels in adipocytes, includes MMP-7 (in subcutaneous fat), MMP-12 and -15 (both in gonadal fat), MMP-19, and TIMP-4 (in both gonadal and subcutaneous fat).

Collectively, these data reveal that in lean mice, mature adipocytes expressed significant mRNA levels of a limited number of MMPs (MMP-12, -15, -19, and -24) and TIMPs (TIMP-3 and -4) and suggested a differential regulation of

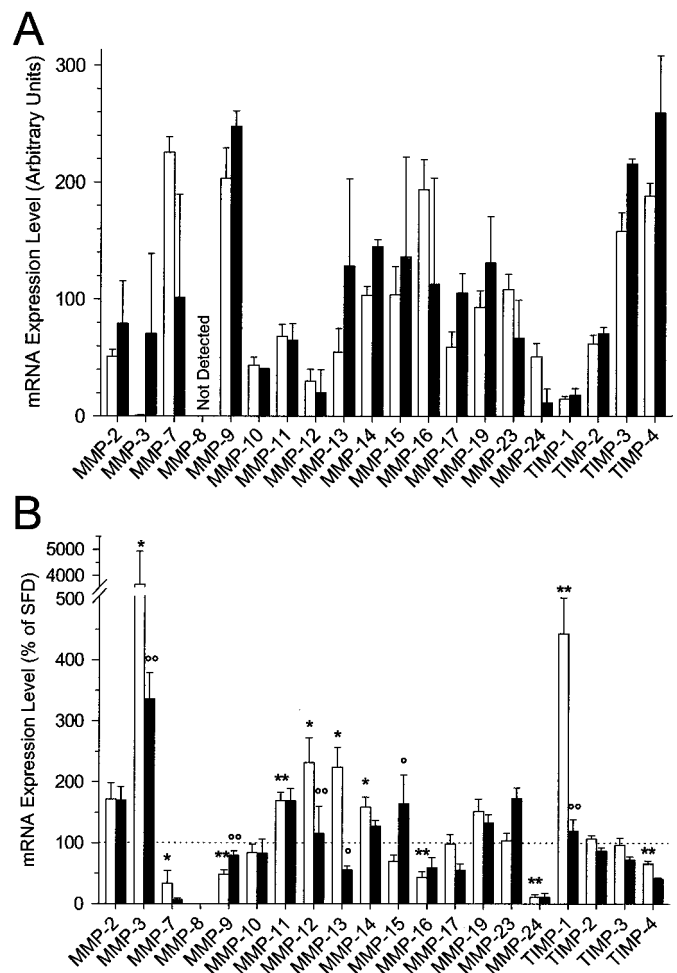


FIG. 1. Expression of MMP and TIMP mRNAs in gonadal and subcutaneous adipose tissue. MMP and TIMP mRNA levels in gonadal (□) and subcutaneous fat pads (■) collected from mice maintained for 15 weeks on SFD (A) or HFD (B) were determined by semiquantitative RT-PCR. Relative expression levels were obtained after normalization for the 28S rRNA levels. Data are means ± SE obtained from the analysis of gonadal fat from mice on SFD ( $n = 6$ ) or HFD ( $n = 6$ ) and subcutaneous fat from mice on SFD ( $n = 2$ ) or HFD ( $n = 6$ ). Results are expressed as normalized mRNA levels (A) or as percent of the expression level observed in mice on SFD (B). \* $P < 0.05$ , \*\* $P < 0.01$  vs. values obtained in gonadal fat from mice on SFD; ° $P < 0.05$ , °° $P < 0.01$  vs. values obtained in gonadal fat from mice on HFD.

TABLE 3  
Expression of MMPs and TIMPs in isolated cells

mRNA species	SFD				HFD			
	Adipocyte		S-V		Adipocyte		S-V	
	GON	SC	GON	SC	GON	SC	GON	SC
MMP-2	+	+	++	++++	-	(+)	+++	++
MMP-3	-	++	+	++++	-	+	+	+++
MMP-7	(+)	+	++++	-	-	-	+++	-
MMP-9	(+)	+	++	+++	-	-	+	++
MMP-10	+	+	+	+++	++	-	++	+++
MMP-11	+	+	+++	+++	-	-	+	+
MMP-12	+++	+	+	++	+++	-	++++	+++
MMP-13	+	+	+++	++	++	-	++++	+++
MMP-14	+	+(+)	++++	++++	+	+	++	+++
MMP-15	++++	++++	+	++++	-	-	++	+++
MMP-16	+	(+)	++++	++++	-	-	++	++(+)
MMP-17	+	++	+++	+++	+	++	++	++
MMP-19	++++	+++	++	++	+	+	++	+(+)
MMP-23	+	+	+++	+++	(+)	-	++	++(+)
MMP-24	+++	++(+)	++++	+++	++	++(+)	++	+++
TIMP-1	+	+	+++	+++	++	+	+++	++(+)
TIMP-2	(+)	(+)	+++	+++	(+)	(+)	++	++
TIMP-3	++	++	+++	++	(+)	+	++	++
TIMP-4	++++	++++	+++	++	++++	+++	++	++
vWF*	21	9	100	100	0.5	3.5	100	100

Mature adipocytes and S-V cells were isolated from mice on SFD or HFD, and mRNA levels were analyzed by semiquantitative RT-PCR. After normalization for 28S rRNA, the expression levels of the different mRNAs were scored on a scale from no (-) to high (++++) expression. \*von Willebrand factor (vWF) was expressed in percent of the expression measured in the corresponding S-V fractions. GON, gonadal; SC, subcutaneous.

the expression of some mRNAs between gonadal and subcutaneous depots (e.g. MMP-3, -7, and -12).

In mice on HFD, the expression profiles in isolated adipocytes and S-V cells were similar to those observed in the SFD groups, except for MMP-15 and -19 mRNAs (Table 3). Indeed, although these two mRNA species were very abundant in adipocytes derived from mice on SFD, their expression was lower in mice on HFD.

#### In situ detection of MMP activities in adipose tissue.

Because MMP activities in tissue are locally determined by the balance between the levels of activated MMPs and their inhibitors, we used in situ fluorescent zymography to demonstrate the presence of MMP-dependent proteolytic activities in intact adipose tissue from mice on HFD. On the casein substrate, lysis corresponded to  $19 \pm 3.4\%$  ( $n = 5$ ) of the section area with subcutaneous tissue and to  $22 \pm 4.1\%$  with gonadal tissue ( $P = \text{NS}$ ); corresponding values on the gelatin substrate were  $8.0 \pm 2.7\%$  and  $6.9 \pm 3.1\%$  ( $n = 5$ ). The addition of EDTA (25 mmol/l) and 1,10-phenanthroline (5 mmol/l) resulted in  $76 \pm 5.6\%$  ( $n = 6$ ) or  $78 \pm 5.5\%$  ( $n = 7$ ) inhibition of lysis on the casein or gelatin substrate gel, respectively.

**Correlations between MMP and TIMP mRNA levels and degree of obesity.** After 15 weeks of either SFD or HFD, the individual total body weights of the mice ranged from 20 to 47 g. A strong positive correlation was observed between total body weight and the weight of either gonadal ( $\rho = 0.95$ ,  $P = 0.000001$ ) or subcutaneous fat ( $\rho = 0.94$ ,  $P = 0.000002$ ), demonstrating that the weight of both depots reflects the extent of obesity. Similar correlation analysis performed for each mRNA species revealed that the levels of MMP-3, -11, -12, -13, and -14 and TIMP-1 were positively correlated with the weight of gonadal fat,

whereas negative correlations were observed for MMP-7, -9, -16, and -24 and TIMP-4 (Table 4). With the exception of MMP-9 and -11, such correlations were not detected in subcutaneous depots.

TABLE 4  
Correlations between MMP and TIMP mRNA levels and the degree of obesity

	GON fat		SC fat	
	$\rho$	$P$	$\rho$	$P$
MMP-2	0.482	0.112	0.683	0.042
MMP-3	<u>0.881</u>	0.0001	0.483	0.187
MMP-7	<u>-0.661</u>	0.019	-0.457	0.215
MMP-9	<u>-0.727</u>	0.007	<u>-0.816</u>	0.007
MMP-10	-0.302	0.315	-0.200	0.606
MMP-11	<u>0.734</u>	0.006	<u>0.750</u>	0.020
MMP-12	<u>0.741</u>	0.006	0.300	0.432
MMP-13	<u>0.685</u>	0.014	0.116	0.765
MMP-14	<u>0.622</u>	0.031	0.366	0.332
MMP-15	-0.461	0.131	0.416	0.264
MMP-16	<u>-0.741</u>	0.004	0.033	0.932
MMP-17	-0.192	0.529	-0.383	0.308
MMP-19	0.286	0.366	0.466	0.205
MMP-23	-0.153	0.633	0.433	0.244
MMP-24	<u>-0.718</u>	0.008	0.217	0.573
TIMP-1	<u>0.780</u>	0.002	0.483	0.187
TIMP-2	0.198	0.517	0.050	0.898
TIMP-3	-0.020	0.948	-0.633	0.067
TIMP-4	<u>-0.708</u>	0.006	<u>-0.533</u>	0.139

Spearman correlation coefficients for the relationships between mRNA levels and the weight of the fat depot in gonadal (GON;  $n = 13$ ) and subcutaneous (SC;  $n = 9$ ) adipose tissue. Statistically significant differences ( $P < 0.05$ ) are underlined.

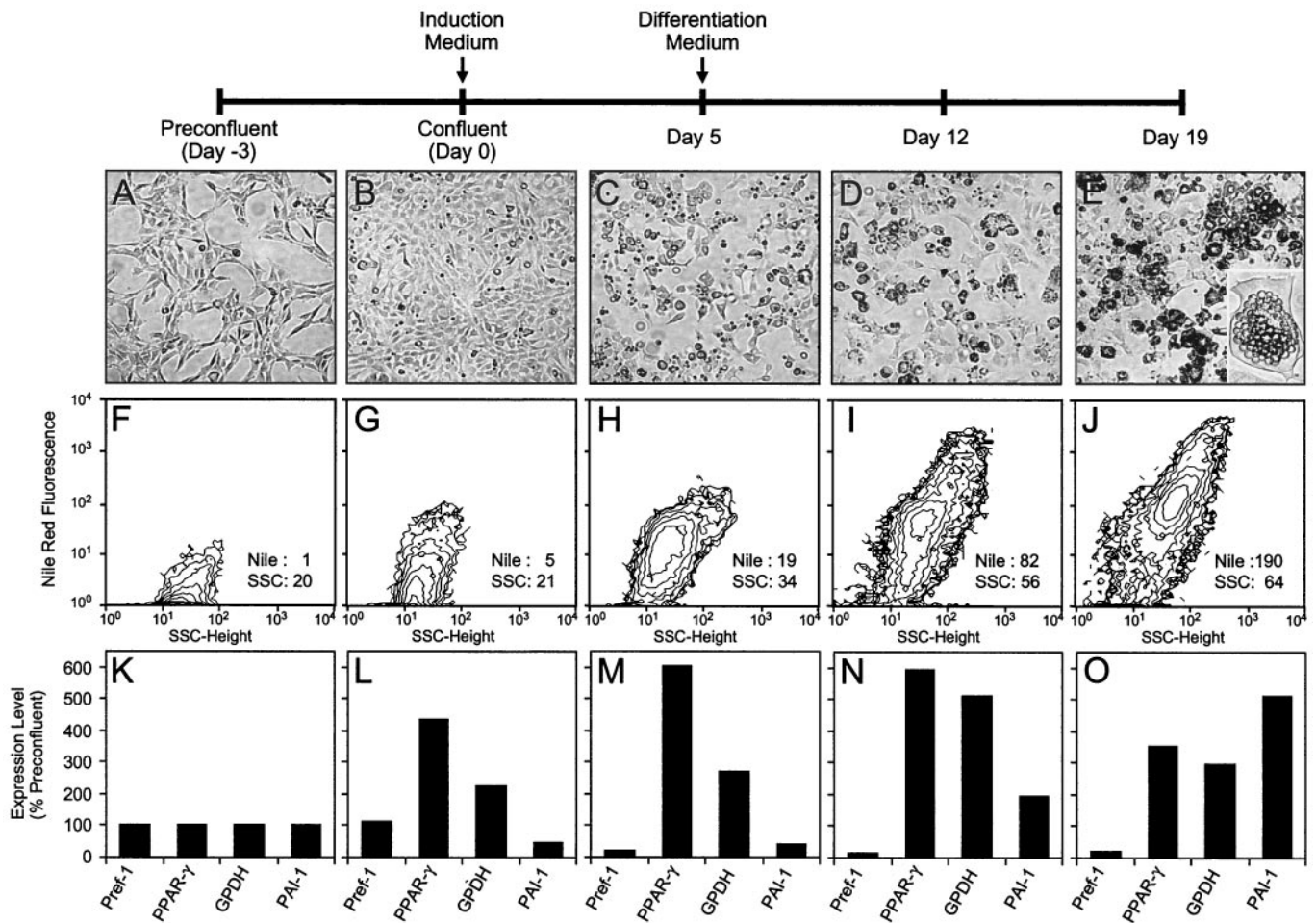


**FIG. 2.** 3T3-F442A preadipocytes as an in vitro model of adipogenesis. 3T3-F442A preadipocytes were cultured in serum-supplemented basal medium until confluence (day 0). Cells were then treated with serum-free induction medium for 5 days and switched to serum-free differentiation medium for 2 weeks. The conversion of preadipocytes into mature lipid-filled adipocytes was characterized by light microscopy (A–E), flow cytometry (F–J), and semiquantitative RT-PCR (K–O) in preconfluent (A, F, K), confluent (B, G, L), 5 days (C, H, M), 12 days (D, I, N), and 19 days (E, J, O) postconfluent cultures. Flow cytometric data are contour plotted according to Nile Red fluorescence, which is indicative of dye uptake into intracellular lipid droplets, and side-scatter (SSC-height) fluorescence, which reflects the cellular morphology. Mean values for Nile Red (Nile) and side-scatter (SSC) fluorescence are indicated. Relative expression levels of preadipocyte factor-1, PPAR- $\gamma$ , GPDH, and PAI-1 were determined by semiquantitative RT-PCR. RT-PCR data are means of two independent experiments and are expressed as a percent of expression level in preconfluent cultures (day 3).

**Modulation of MMP and TIMP expression during in vitro adipogenesis.** We used 3T3-F442A preadipocytes as an in vitro model of adipogenesis. Confluent cultures (day 0) were incubated with an induction medium containing insulin, dexamethasone, methylisobutylxanthine, and  $T_3$  until day 5 and then maintained in a differentiation medium (insulin and  $T_3$ ) for 2 weeks. This treatment induced adipogenesis in a large percentage of the cells. The differentiation was characterized by the conversion of preadipocytes (Fig. 2A) into spherical lipid-filled adipocytes (Fig. 2E, insert). To monitor adipogenesis, flow cytometric analyses were performed during the differentiation process (Fig. 2F–J). Preadipocyte differentiation resulted in the appearance of a population of cells characterized by higher intensities of both Nile Red and side-scatter fluorescences (compare Fig. 2A–E with 2F–J). Early signs of differentiation were detected in untreated confluent cultures (day 0), as judged from the presence of small amounts of intracellular lipids (Fig. 2B and G) and by increased levels of peroxisome proliferator-activated receptor (PPAR)- $\gamma$  mRNA, a marker of early differentiation,

and glycerophosphate dehydrogenase (GPDH) mRNA, a marker of the terminal phase of differentiation (Fig. 2L). Treatment of confluent preadipocytes with the induction medium resulted in a 80% decrease of preadipocyte factor-1, a marker of preadipocytes, mRNA level (Fig. 2M) that was concomitant with a strong induction of PPAR- $\gamma$  expression. As differentiation proceeded, GPDH expression increased simultaneously with the accumulation of intracellular lipids (Fig. 2D, I, and N). After 19 days, numerous lipid-filled adipocytes, characterized by lower PPAR- $\gamma$  and GPDH but high PAI-1 (a molecule expressed at higher levels in fully differentiated adipocytes [21]) mRNA levels (Fig. 2E, J, and O), were observed.

Quantification of MMP and TIMP mRNA levels revealed different expression profiles (Fig. 3A). mRNAs for MMP-2, -3, -7, -10, -11, -12, and -13 increased throughout the differentiation process and were maximal in mature adipocytes (between days 12 and 19), as observed for PAI-1 (Fig. 2K–O). mRNAs for MMP-9 and -16 and TIMP-1 were high in preconfluent cultures, decreased during early differentiation, and increased as adipocytes matured. mRNAs

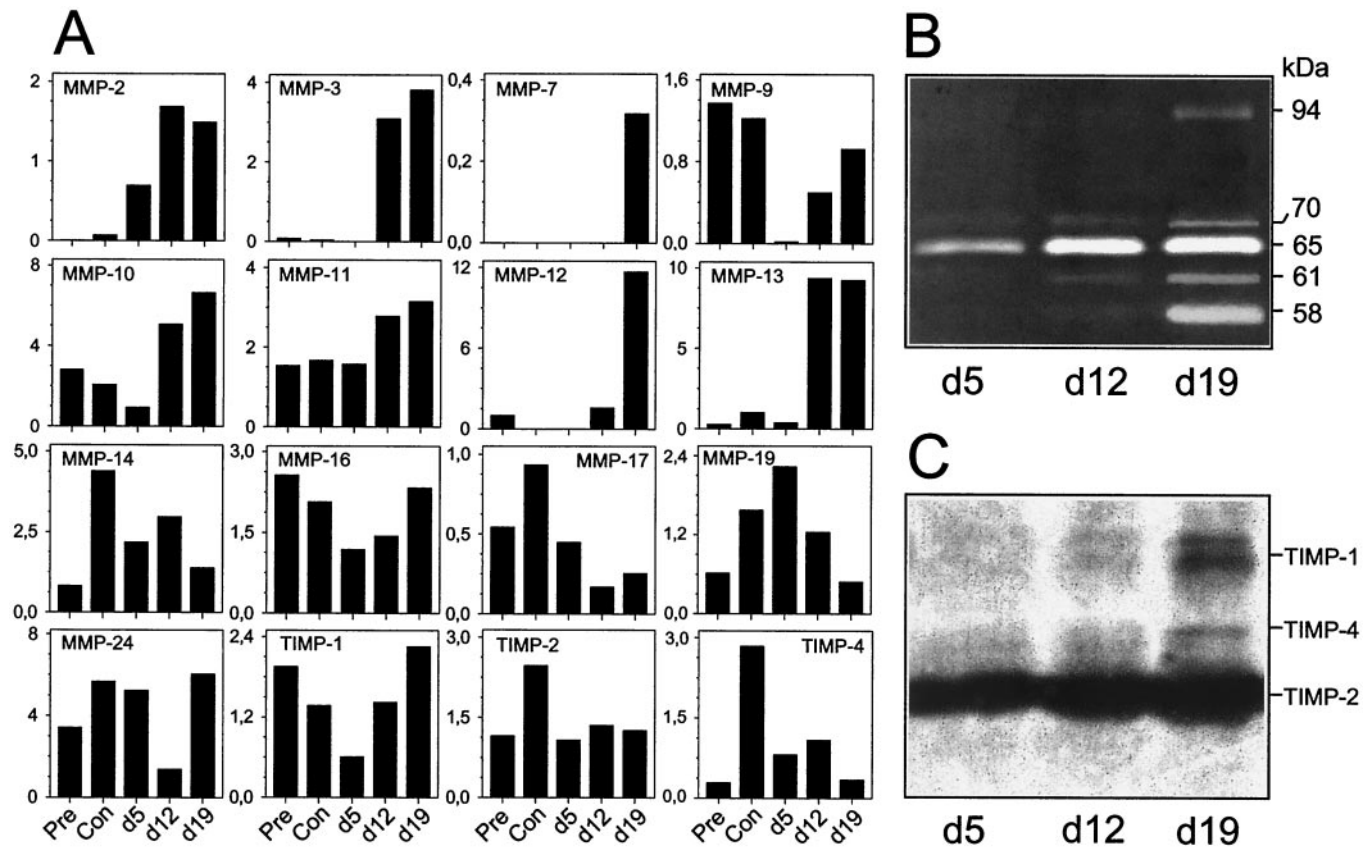


**FIG. 3.** Expression of MMPs and TIMPs during in vitro adipogenesis. **A:** Total RNA was extracted from 3T3-F442A cells at different stages of differentiation: pre, preconfluent; con, confluent (day 0); d5, d12, and d19, postconfluent cultures after 5, 12, and 19 days, respectively. RNA samples were analyzed for MMP and TIMP mRNA levels by semiquantitative RT-PCR. Data were expressed as relative expression levels obtained after normalization for the 28S rRNA levels. Secretion of MMPs and TIMPs by differentiating adipocytes into the serum-free culture medium was analyzed by gelatin zymography (**B**) and reverse zymography (**C**), respectively.

for MMP-14, -17, and -19 and TIMP-2 and -4 peaked early and then later decreased during differentiation. mRNAs for MMP-15 and -23 were expressed at very-low levels. MMP-8 and TIMP-3 mRNAs were not detected.

Measurement of MMP and TIMP secretion during the differentiation process was performed by gelatin zymography and reverse zymography (Fig. 3B and C). Latent pro-MMP-2 (70- and 65-kDa bands) was the major proteolytic enzyme detected by gelatin zymography. Its secretion as well as its processing into active lower molecular weight forms (61 and 58 kDa) were both increased during differentiation. By day 19, an additional gelatinolytic activity of 94 kDa, corresponding to MMP-9, was observed. Analysis of concentrated media by reverse zymography revealed the presence of three TIMP activities (Fig. 3C). Based on their apparent molecular sizes, these were most likely TIMP-1 at a molecular weight of 30,000, TIMP-3 and/or -4 at a molecular weight of 23,000, and TIMP-2 at a molecular weight of 20,000. Because of the absence of detectable TIMP-3 mRNA in these cells, the inhibitory activity of 23 kDa presumably corresponds to TIMP-4.

**Inhibition of in vitro adipogenesis by a synthetic MMP inhibitor.** When confluent 3T3-F442A cultures were differentiated in the presence of 10  $\mu\text{mol/l}$  CT1746 (a synthetic hydroxamate-based MMP inhibitor), flow cytometric analysis revealed an inhibition of lipid accretion (Fig. 4). The inhibitor did not alter cellular viability, as assessed by cell counting, Trypan Blue dye exclusion, and

WST-1 assay (data not shown), thus ruling out a potential cytotoxic effect. Analysis of culture supernatants by gelatin zymography did not reveal any modulation of MMP secretion by this inhibitor (data not shown). Addition of CT1746 (10  $\mu\text{mol/l}$ ) to the incubation buffer completely abolished the lysis zones on the gels, confirming the inhibitory activity of this compound (data not shown).

## DISCUSSION

In this study, we investigated the expression of 16 MMPs and 4 TIMPs in the fat pads of mice maintained for 15 weeks on SFD or HFD. Except for MMP-8, all MMP and TIMP mRNAs analyzed were detected in both gonadal and subcutaneous depots. Mature adipocytes, the major component of the adipose tissue, expressed a limited number of these transcripts, including MMP-12, -15, -19, and -24 and TIMP-3 and -4. However, the presence of contaminating endothelial cells in the adipocyte fractions (especially those isolated from mice on SFD) might have affected the expression profiles depicted in Table 3. Nevertheless, a comparison with the expression profiles observed in adipocytes isolated from mice on HFD, which contain extremely low levels of contaminating cells, indicated that mature adipocytes expressed at least MMP-12 (in gonadal fat), MMP-24, and TIMP-4. The expression of MMP-15 and MMP-19, which were high in adipocytes derived from mice on SFD, was extremely low or undetectable in adipocytes

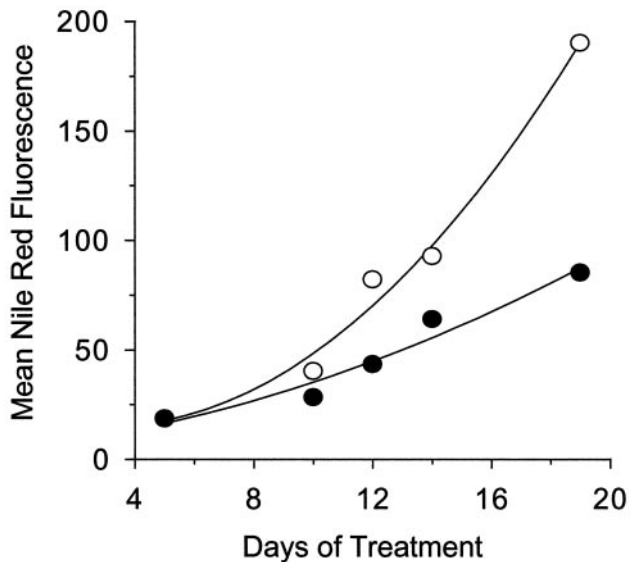


**FIG. 4.** Inhibition of *in vitro* adipogenesis by a synthetic MMP inhibitor. Adipocyte differentiation was performed in the presence of a synthetic MMP inhibitor. At day 0 of the differentiation process, confluent 3T3-F442A cells were treated with vehicle (○) or CT1746 (●, 10  $\mu$ mol/l) for 19 days. Adipocyte differentiation was monitored by flow cytometry, and data were expressed as mean Nile Red fluorescence. Results shown are representative of two independent experiments.

from mice on HFD, suggesting that the expression of these mRNAs was either endothelial-specific or downregulated in mature adipocytes when the mice received an HFD. In contrast, stromal cells, which comprise preadipocytes, fibroblasts, and blood vessels, expressed all MMP and TIMP mRNAs.

In agreement with earlier studies (22), feeding the mice an HFD led to the development of obesity. Nutritionally induced obese mice showed a higher total body weight, larger fat pads, and hypertrophic adipocytes. In addition to these morphological changes, MMP and TIMP expression profiles were profoundly altered. The mRNA levels of MMP-3, -11, -12, -13, and -14 and TIMP-1 were upregulated, whereas MMP-7, -9, -16, and -24 and TIMP-4 were downregulated. Most of these modulations were specific to the gonadal fat (Table 4), supporting the concept that the different depots are not identical (23). Such regional variations in the regulation of MMPs could arise from differences in cellular composition (e.g., gonadal fat contains more S-V cells than subcutaneous fat) and/or from regional differences in the secretion of proteins such as interleukin-6 or leptin (24), which can affect MMP expression (25).

The catalytic activity of MMPs is tightly regulated and primarily determined by the balance between the levels of activated MMPs and TIMPs. Using fluorescent *in situ* zymography, we were able to detect MMP-dependent proteolytic activities in intact adipose tissue. Moreover, daily injection of mice maintained on an HFD with galardin (a synthetic broad spectrum MMP inhibitor) resulted in lower MMP-mediated proteolytic activities in fat pads (H.R.L., E.M., L.B. Hansen, B. Van Hoef, L. Frederix, and D.C., unpublished observation). Collectively, these data demonstrated that *in situ*, the level of active MMPs exceeded the level of inhibitors.

Obesity has been associated with an extensive reorga-

nization of the adipose tissue involving adipogenesis, angiogenesis, and ECM remodeling. A large body of evidence has established that the ECM not only functions as a structural support but also influences cell-cell interactions, differentiation, and migration. Such functions may be necessary for the cellular reorganization of fat pads as well as for regulation of the expression of adipocyte genes. Although several reports have demonstrated that ECM components influence adipocyte differentiation *in vitro*, few of them have addressed the potential contribution of ECM remodeling.

Because of the pleiotropic functions attributed to MMPs and TIMPs, it is likely that these molecules affect several cellular processes in the fat depots. Indeed, MMPs are collectively able to cleave a wide variety of substrates, including ECM components, proteinases and inhibitors, matrix receptors, and receptors involved in cell-cell interactions (26). These functions suggest that MMPs could facilitate adipose tissue remodeling by increasing matrix plasticity. Moreover, adipocytes are surrounded by a basement membrane (27) that has to be extensively remodeled in order to allow the hypertrophic development of adipocytes observed in obesity. In agreement with this hypothesis, MMP-2 and -9, two major MMPs implicated in basement membrane remodeling, were detected in murine (28) and human mature adipocytes (29). MMPs can also release, activate, or degrade several growth factors and cytokines (26) implicated in obesity. MMPs also play major roles in angiogenesis (30), an essential process for the development of adipose tissue (6).

Formation of adipose tissue requires the conversion of preadipocytes into mature adipocytes (31). This differentiation switch activates a new program of gene expression that is followed by the accumulation of lipids. We therefore examined the pattern of MMP and TIMP expression during adipocyte differentiation, using 3T3-F442A preadipocytes as an *in vitro* model of adipogenesis. It was previously shown that differentiation of 3T3 preadipocytes mimics the *in vivo* process, yielding cells expressing many of the same genes as well as morphological and metabolic characteristics of *in vivo* adipocytes (32,33).

Our data show that most MMP and TIMP transcripts detected *in vivo* were also expressed and modulated *in vitro* during differentiation. However, the comparison of the patterns of gene expression between *in vitro* differentiated adipocytes (Fig. 3) and isolated mature adipocytes (Table 3) revealed some discrepancies. Whereas MMP-2, -9, -11, and -16 and TIMP-2 mRNAs were expressed in *in vitro* differentiated adipocytes, they were not detected in isolated mature adipocytes. These discrepancies likely result from the uncompleted differentiation observed *in vitro*. Indeed, although a homogenous population of mature adipocytes was isolated from the fat pads, *in vitro* adipogenesis generated a mixture of cells at different stages of differentiation. Furthermore, adipocytes generated *in vitro* displayed a multilocular morphology that differed from the unilocular adipocytes observed *in vivo*. In agreement with these observations, recent reports demonstrated that the changes in gene expression associated with adipocyte development *in vivo* and *in vitro*, though overlapping, may be different in some respects (33,34).

Differentiation of 3T3-F442A cells was also associated with the deposition of an abundant ECM (data not shown) and the secretion of MMP-2 and -9. When the differentiation procedure was performed in the presence of CT1746, a synthetic MMP inhibitor that has a greater specificity for MMP-2, -3, and -9 than for MMP-7 (35), the accumulation of intracytoplasmic lipids was reduced, demonstrating the implication of MMPs during adipogenesis. Nevertheless, we cannot exclude the possibility that this synthetic inhibitor may also influence adipogenesis by interfering with other metalloproteinases such as the adamalysins. Interestingly, when mice maintained on HFD for up to 12 weeks were daily injected with galardin, another synthetic MMP inhibitor, a significant reduction of both gonadal and subcutaneous fat pad weights was observed, although the total body weight remained unchanged (H.R.L., E.M., L.B. Hansen, B. Van Hoef, L. Frederix, and D.C., unpublished observation). This observation further supports the hypothesis that the catalytic activity of MMPs is important for adipose tissue development.

In contrast with our data, Alexander et al. (36) recently reported an accelerated lipogenesis in differentiating 3T3-L1 adipocytes treated with TIMP-1 or GM6001, a broad spectrum MMP inhibitor. These conflicting observations might arise from differences in experimental models (3T3-L1 vs. 3T3-F442A cells), differentiation procedure (serum-containing versus serum-free medium in current study), and/or specificity of the inhibitors.

In conclusion, we have revealed that a large array of MMPs and TIMPs are expressed in murine adipose tissue as well as in differentiating 3T3-F442A preadipocytes. The striking modulations of their expression in a model of nutritionally induced obesity as well as their involvement during *in vitro* adipogenesis suggest a functional role for MMPs and TIMPs in the pathophysiology of the adipose tissue.

#### ACKNOWLEDGMENTS

This study was supported by a grant from the Interuniversity Attraction Poles (Belgium).

The skillful technical assistance of A. De Wolf, G. Lemmens, and B. Van Hoef is gratefully acknowledged.

#### REFERENCES

- Ahima RS, Flier JS: Adipose tissue as an endocrine organ. *Trends Endocrinol Metab* 11:327–332, 2000
- Himms-Hagen J: Obesity may be due to a malfunctioning of brown fat. *Can Med Assoc J* 121:1361–1364, 1979
- Lowell BB, S-Susulic V, Hamann A, Lawitts JA, Himms-Hagen J, Boyer BB, Kozak LP, Flier JS: Development of obesity in transgenic mice after genetic ablation of brown adipose tissue. *Nature* 366:740–742, 1993
- Kahn BB, Flier JS: Obesity and insulin resistance. *J Clin Invest* 106:473–481, 2000
- Kopelman PG: Obesity as a medical problem. *Nature* 404:635–643, 2000
- Crandall DL, Hausman GJ, Kral JG: A review of the microcirculation of adipose tissue: anatomic, metabolic, and angiogenic perspectives. *Microcirculation* 4:211–232, 1997
- Carmeliet P, Collen D: Development and disease in proteinase-deficient mice: role of the plasminogen, matrix metalloproteinase and coagulation system. *Thromb Res* 91:255–285, 1998
- Loskutoff DJ, Samad F: The adipocyte and hemostatic balance in obesity: studies of PAI-1. *Arterioscler Thromb Vasc Biol* 18:1–6, 1998
- Alessi MC, Bastelica D, Morange P, Berthet B, Leduc I, Verdier M, Geel O, Juhan-Vague I: Plasminogen activator inhibitor 1, transforming growth factor-beta1, and BMI are closely associated in human adipose tissue during morbid obesity. *Diabetes* 49:1374–1380, 2000
- Chambers AF, Matrisian LM: Changing views of the role of matrix metalloproteinases in metastasis. *J Natl Cancer Inst* 89:1260–1270, 1997
- Noel A, Gilles C, Bajou K, Devy L, Kebers F, Lewalle JM, Maquoi E, Munaut C, Remacle A, Foidart JM: Emerging roles for proteinases in cancer. *Invasion Metastasis* 17:221–239, 1997
- Hidalgo M, Eckhardt SG: Development of matrix metalloproteinase inhibitors in cancer therapy. *J Natl Cancer Inst* 93:178–193, 2001
- Nagase H, Woessner JF: Matrix metalloproteinases. *J Biol Chem* 274:21491–21494, 1999
- Gomez DE, Alonso DF, Yoshiji H, Thorgeirsson UP: Tissue inhibitors of metalloproteinases: structure, regulation and biological functions. *Eur J Cell Biol* 74:111–122, 1997
- Giles AR: Guidelines for the use of animals in biomedical research. *Thromb Haemost* 58:1078–1084, 1987
- Galis ZS, Sukhova GK, Libby P: Microscopic localization of active proteases by *in situ* zymography: detection of matrix metalloproteinase activity in vascular tissue. *FASEB J* 9:974–980, 1995
- Rodbell M: Metabolism of isolated fat cells. I. Effects of hormones on glucose metabolism and lipolysis. *J Biol Chem* 239:375–380, 1964
- Maquoi E, Noel A, Frankenne F, Anglikier H, Murphy G, Foidart JM: Inhibition of matrix metalloproteinase 2 maturation and HT1080 invasiveness by a synthetic furin inhibitor. *FEBS Lett* 424:262–266, 1998
- Remacle AG, Baramova EN, Weidle UH, Krell HW, Foidart JM: Purification of progelatinases A and B by continuous-elution electrophoresis. *Protein Expr Purif* 6:417–422, 1995
- Crandall DL, Armellino DC, Busler DE, McHendry-Rinde B, Kral JG: Angiotensin II receptors in human preadipocytes: role in cell cycle regulation. *Endocrinology* 140:154–158, 1999
- Samad F, Yamamoto K, Loskutoff DJ: Distribution and regulation of plasminogen activator inhibitor-1 in murine adipose tissue *in vivo*: induction by tumor necrosis factor-alpha and lipopolysaccharide. *J Clin Invest* 97:37–46, 1996
- Schreyer SA, Wilson DL, LeBoeuf RC: C57BL/6 mice fed high fat diets as models for diabetes-accelerated atherosclerosis. *Atherosclerosis* 136:17–24, 1998
- Dusserre E, Moulin P, Vidal H: Differences in mRNA expression of the proteins secreted by the adipocytes in human subcutaneous and visceral adipose tissues. *Biochim Biophys Acta* 1500:88–96, 2000
- Arner P: Regional differences in protein production by human adipose tissue. *Biochem Soc Trans* 29:72–75, 2001
- Park HY, Kwon HM, Lim HJ, Hong BK, Lee JY, Park BE, Jang Y, Cho SY, Kim HS: Potential role of leptin in angiogenesis: leptin induces endothelial cell proliferation and expression of matrix metalloproteinases *in vivo* and *in vitro*. *Exp Mol Med* 33:95–102, 2001
- McCawley LJ, Matrisian LM: Matrix metalloproteinases: multifunctional contributors to tumor progression. *Mol Med Today* 6:149–156, 2000
- Pierleoni C, Verdenelli F, Castellucci M, Cinti S: Fibronectins and basal lamina molecules expression in human subcutaneous white adipose tissue. *Eur J Histochem* 42:183–188, 1998
- Lijnen HR, Maquoi E, Holvoet P, Mertens A, Lupu F, Morange P, Alessi MC, Juhan-Vague I: Adipose tissue expression of gelatinases in mouse models of obesity. *Thromb Haemost* 85:1111–1116, 2001
- Bouloumié A, Sengenès C, Portolan G, Galitzky J, Lafontan M: Adipocyte produces matrix metalloproteinases 2 and 9: involvement in adipose differentiation. *Diabetes* 50:2080–2086, 2001
- Stetler-Stevenson WG: Matrix metalloproteinases in angiogenesis: a moving target for therapeutic intervention. *J Clin Invest* 103:1237–1241, 1999
- Smas CM, Sul HS: Control of adipocyte differentiation. *Biochem J* 309:697–710, 1995
- MacDougald OA, Lane MD: Transcriptional regulation of gene expression during adipocyte differentiation. *Annu Rev Biochem* 64:345–373, 1995
- Soukas A, Succi ND, Saatkamp BD, Novelli S, Friedman JM: Distinct transcriptional profiles of adipogenesis *in vivo* and *in vitro*. *J Biol Chem* 276:34167–34174, 2001
- Nadler ST, Stoehr JP, Schueler KL, Tanimoto G, Yandell BS, Attie AD: The expression of adipogenic genes is decreased in obesity and diabetes mellitus. *Proc Natl Acad Sci U S A* 97:11371–11376, 2000
- An Z, Wang X, Willmott N, Chander SK, Tickle S, Docherty AJ, Mountain A, Millican AT, Morphy R, Porter JR, Epemolu RO, Kubota T, Moossa AR, Hoffman RM: Conversion of highly malignant colon cancer from an aggressive to a controlled disease by oral administration of a metalloproteinase inhibitor. *Clin Exp Metastasis* 15:184–195, 1997
- Alexander CM, Selvarajan S, Mudgett J, Werb Z: Stromelysin-1 regulates adipogenesis during mammary gland involution. *J Cell Biol* 152:693–703, 2001